THE JOURNAL OF BIOLOGICAL CHEMISTRY VOL. 287, NO. 32, pp. 26596–26605, August 3, 2012

Lethal, Hereditary Mutants of Phospholamban Elude Phosphorylation by Protein Kinase A*

Received for publication, May 17, 2012, and in revised form, June 13, 2012 Published, JBC Papers in Press, June 15, 2012, DOI 10.1074/jbc.M112.382713

Delaine K. Ceholski[‡1], **Catharine A. Trieber**[‡§], **Charles F. B. Holmes**[‡], **and Howard S. Young**[‡§2]

From the [‡]*Department of Biochemistry, University of Alberta, Edmonton, Alberta T6G 2H7, Canada and the* [§]*National Institute for Nanotechnology, University of Alberta, Edmonton, Alberta T6G 2M9, Canada*

Background: Heterozygous mutations in the cytoplasmic domain of phospholamban cause lethal dilated cardiomyopathy.
Results: The mutations alter phospholamban-protein kinase A interactions that are essential for substrate recognition and phosphorylation.
Conclusion: Hereditary mutations in phospholamban that prevent phosphorylation by protein kinase A will lead to chronic inhibition of SERCA.
Significance: Arginines in the cytoplasmic domain of phospholamban should be considered hot spots for hereditary mutations leading to dilated cardiomyopathy.

The sarcoplasmic reticulum calcium pump (SERCA) and its regulator, phospholamban, are essential components of cardiac contractility. Phospholamban modulates contractility by inhibiting SERCA, and this process is dynamically regulated by β-adrenergic stimulation and phosphorylation of phospholamban. Herein we reveal mechanistic insight into how four hereditary mutants of phospholamban, Arg^9 to Cys, Arg^9 to Leu, Arg^9 to His, and Arg^{14} deletion, alter regulation of SERCA. Deletion of Arg^{14} disrupts the protein kinase A recognition motif, which abrogates phospholamban phosphorylation and results in constitutive SERCA inhibition. Mutation of Arg^9 causes more complex changes in function, where hydrophobic substitutions such as cysteine and leucine eliminate both SERCA inhibition and phospholamban phosphorylation, whereas an aromatic substitution such as histidine selectively disrupts phosphorylation. We demonstrate that the role of Arg^9 in phospholamban function is multifaceted: it is important for inhibition of SERCA, it increases the efficiency of phosphorylation, and it is critical for protein kinase A recognition in the context of the phospholamban pentamer. Given the synergistic consequences on contractility, it is not surprising that the mutants cause lethal, hereditary dilated cardiomyopathy.

In cardiac muscle, β-adrenergic stimulation increases contractility and accelerates relaxation. These effects are due to the activation of PKA, which targets a variety of downstream contractile and calcium-handling systems. One such target is phospholamban (PLN),[3] a regulator of the sarcoplasmic reticulum calcium pump (SERCA) (1). Following an appropriate physiological cue, PKA phosphorylates PLN and increases calcium reuptake by SERCA into the sarcoplasmic reticulum (SR). Although the role of SERCA and PLN in muscle relaxation is clear, evidence from animal models suggests that most of the inotropic effects on contractility also originate from SR calcium handling (2). This is because dynamic control of myocardial contraction-relaxation involves fine tuning SERCA inhibition and SR calcium levels. SERCA function depends on the available pool of inhibitory PLN, which in turn depends on the cytosolic calcium concentration and the oligomeric and phosphorylation states of PLN (1, 3). It is known that defects at any point in this pathway can result in heart failure (4), although it took almost three decades after the initial discovery of PLN to establish this link.

Dilated cardiomyopathy (DCM) is a major cause of cardiovascular disease, with ~30% of cases being of familial or hereditary origin (5). Many disease-causing mutations are found in genes encoding contractile or calcium-handling proteins, such as PLN, where defects in force transmission, endoplasmic reticulum stress, apoptosis, and biomechanical stress underlie the development and progression of DCM. In humans, abnormal SERCA to PLN ratios (6–8) or mutations in PLN (9–12) are associated with disease, whereas superinhibitory and chronically inhibitory PLN mutations can cause heart failure in mouse models (13–15). Two such examples of mutations include R9C and Arg^{14} deletion (R14del) in the cytoplasmic domain of PLN (9, 11), which have been linked to DCM in extended family pedigrees. In addition, R9L and R9H are newly identified mutations, although their linkage to heart failure has not been fully established (12). These hereditary mutations are somewhat surprising because Arg^9 and Arg^{14} were not previously considered essential residues of PLN, and overall the cytoplasmic domain of PLN makes a small contribution to SERCA inhibition (16). Nonetheless, cysteine substitution of Arg^9 is thought to result in loss of inhibitory function and trapping of PKA, whereas deletion of Arg^{14} alters the PKA recognition motif of PLN. The resultant effects on SERCA function and SR calcium stores are causative in the development and progression of DCM.

* This work was supported by Canadian Institutes of Health Research Grant MOP53306.
[1] Supported by Canadian Institutes of Health Research and Alberta Innovates Technology Futures.
[2] Senior Scholar of Alberta Innovates Health Solutions. To whom correspondence should be addressed: 327 Medical Sciences Bldg., University of Alberta, Edmonton, AB T6G 2H7, Canada. Tel.: 780-492-3931; Fax: 780-492-0886; E-mail: hyoung@ualberta.ca.
[3] The abbreviations used are: PLN, phospholamban; SERCA, sarco(endo)plasmic reticulum calcium ATPase; DCM, dilated cardiomyopathy; SR, sarcoplasmic reticulum; PKA-c, catalytic subunit of PKA.

To gain mechanistic insight into R9C, R9L, R9H, and R14del, we created missense and deletion mutants in the cytoplasmic domain of PLN and characterized their effects on phosphorylation by PKA in the absence and presence of SERCA. For the disease-associated mutants, R14del resulted in a slight loss of inhibitory function and a complete loss of phosphorylation, R9H resulted in normal inhibitory function and a complete loss of phosphorylation, and R9L and R9C resulted in a complete loss of both inhibitory function and phosphorylation. Any changes to the PKA recognition motif of PLN (Arg^{13}-Arg^{14}-Ala^{15}-Ser^{16}) (3, 17) eliminated phosphorylation, providing a simple explanation for the R14del mutant. That is, deletion of Arg^{14} would be expected to render PLN unresponsive to β-adrenergic stimulation and constitutively active as an inhibitor of SERCA. In contrast, mutagenesis of Arg^{9} revealed multiple effects on SERCA regulation (18). All nonconservative mutations of Arg^{9} significantly decreased the inhibitory activity of PLN, as well as its ability to be phosphorylated by PKA. Further insight was gained through the mutagenesis of PKA, which revealed that Glu^{203} and Asp^{241} were required for efficient phosphorylation of PLN. By virtue of an electrostatic interaction with Arg^{9} of PLN, these PKA residues increase the efficiency of phosphorylation and allow PKA to recognize PLN in the context of the pentamer. To summarize our findings, Arg^{9} of PLN plays a multifaceted role in cardiac contractility: it is important for SERCA inhibition, it increases the efficiency of PLN phosphorylation, and it allows PKA to recognize nonphosphorylated PLN monomers in the context of a partially phosphorylated pentamer.

EXPERIMENTAL PROCEDURES

Sample Preparation—SERCA1a was prepared from rabbit hind leg muscle (19, 20), and recombinant human PLN was made using established procedures (18, 21). SERCA and PLN were reconstituted for functional assays using established procedures (22, 23) to obtain final molar ratios of 1 SERCA to 4.5 PLN to 120 lipids. ATPase assays were performed as previously described (18, 24). For phosphorylation assays, a "fast" reconstitution was performed to increase the lipid to protein ratio of the co-reconstituted proteoliposomes (25). The final molar ratios were 1 SERCA to 4.5 PLN to 900 lipids. For all proteoliposomes used herein, the concentrations of SERCA and PLN were determined by quantitative SDS-PAGE (26).

Phosphorylation Assays—PLN was first phosphorylated in detergent solution by the catalytic subunit of PKA (PKA-c) (Sigma-Aldrich) in the absence of SERCA as previously described (22) with a molar stoichiometry of 1 PKA-c to 1000 PLN. PLN was phosphorylated with ATP spiked with [γ-^{32}P]ATP (~0.1 μCi/μl). All other components of the reaction were identical to published protocols (22). The reactions were stopped by the addition of TCA, incubated on ice for 10 min, washed several times with 10% TCA and water, and counted in 1 ml of liquid scintillant (Perkin-Elmer) for 1 min in a scintillation counter. All of the values were corrected by subtracting background counts per minute from samples containing no PKA.

PLN was also phosphorylated by PKA-c in co-reconstituted proteoliposomes in the presence of SERCA (50 μl) as previously described (22) with a molar stoichiometry of 1 PKA-c to 50 PLN. The ATP was spiked with [γ-^{32}P]ATP (~0.1 μCi/μl), and the samples were treated as described above. All of the values were corrected for PLN concentration in proteoliposomes as determined by gel quantitation (ImageQuant software; GE Healthcare).

Recombinant PKA Purification—The wild-type bovine PKA catalytic subunit cloned into the pET3a vector (EMD Chemicals, San Diego, CA) was purchased from Biomatik (Cambridge, Canada). Codons were optimized for expression in *Escherichia coli* and a six-histidine tag was added on the N terminus of the PKA gene. The plasmid was transformed into *E. coli* (DE_3) pLysS cells (Stratagene, Santa Clara, CA). Cultures were grown at 37 °C in noninducible minimal media (MDAG-135) (27) until A_{600} = 0.6 and then induced with IPTG (0.5 mM) for 6 h at 22 °C. Recombinant PKA was purified on a nickel-nitrilotriacetic acid column (Qiagen) under native conditions according to the protocol provided in the Qiaexpressionist (Qiagen). After elution, recombinant PKA was concentrated (~1 mg/ml) and dialyzed into 50 mM Tris-HCl, pH 7.5, 50 mM NaCl, 0.2% β-mercaptoethanol, 50% glycerol, and 1 mM EDTA. This protocol was repeated for the E203A and D241A mutants of PKA. The purity and concentration of each mutant was assessed by SDS-PAGE, and all activity values were corrected for it.

Kemptide and PLN Peptide Phosphorylation—The kinetic values for the PKA proteins were acquired from a [γ-^{32}P]ATP phosphorylation filter binding assay that has been previously described (28). Kemptide was purchased from Promega, and PLN cytoplasmic peptides were synthesized by Biomatik Corporation. Kemptide and wild-type PLN peptide concentrations were varied from 1.0 to 400 μM for wild-type PKA and 1 to 700 μM for E203A and D241A PKA; R9C PLN peptide was only varied from 1 to 300 μM for wild-type and mutant PKAs because of solubility problems. K_m and V_{max} were obtained by fitting the data to the Michaelis-Menten equation ($v = V_{max}[S]/([S]+K_m)$), and all of the data were plotted as substrate concentration (μM) *versus* activity (μM/min).

PLN Phosphorylation with Recombinant PKA—Detergent-solubilized wild-type and R9S PLN (0.15 mM) were phosphorylated for 0, 5, 15, 30, 45, and 60 min as described above under phosphorylation assays (molar ratio of 1 PKA to 1000 PLN).

RESULTS

Functional Properties of PLN Mutants Implicated in Hereditary Cardiac Pathology—Although the root cause of DCM can be a single site mutation in PLN, heart failure is an incredibly complex process that impairs many aspects of calcium homeostasis and the cellular proteome, including decreased levels of SERCA (29, 30). Mechanistically, it is important to separate initiating events from the complex array of secondary pathological consequences that define heart failure. Hereditary missense mutations, such as those found in PLN, provide valuable insights into disease-associated changes in calcium homeostasis. In the case of PLN mutants (R9C, R9H, R9L, and R14del), SERCA dysregulation accounts for the earliest stages of disease, which ultimately leads to reduced pumping force, cardiovascular remodeling, and heart failure.

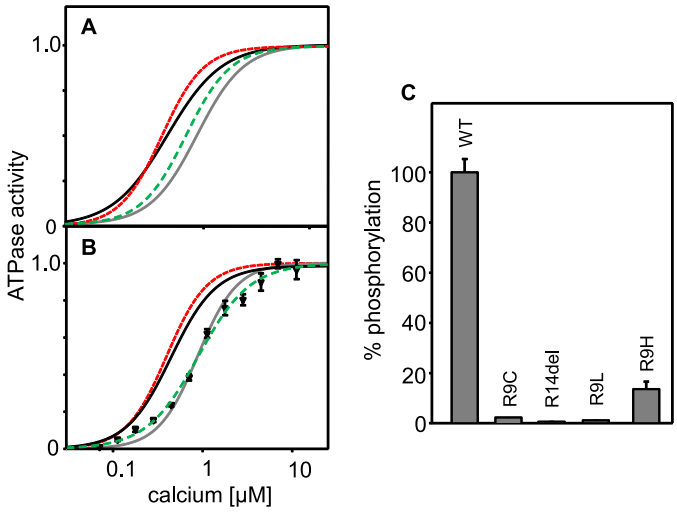

FIGURE 1. **Fitted curves of normalized ATPase activity as a function of calcium concentration for SERCA reconstitutions were adapted from Ceholski *et al.* (18) and are shown for comparison with R9H PLN data ± S.E. (▼, $n = 9$).** *A* and *B*, SERCA was reconstituted in the absence (*black curve*) and presence of wild-type PLN (*gray curve*) or R9C (*red curve*) or R14del (*green curve*) (*A*) or R9L (*red curve*) or R9H (*green curve*) PLN (*B*). All kinetic values are given in Table 1. *C*, PKA-mediated phosphorylation of wild-type and disease-associated mutants of PLN. Phosphorylation is shown as a percentage of wild-type PLN ± S.E. (100% = complete phosphorylation) ($n \geq 4$).

TABLE 1
Kinetic parameters from Hill plots and phosphorylation of disease-associated PLN mutations

	V_{max}	K_{Ca}	Phosphorylation[a]
	μmol min^{-1} *mg*$^{-1}$	*μM*	*%*
SERCA[b]	4.1 ± 0.1	0.46 ± 0.02	
wt-PLN[b]	6.1 ± 0.1	0.88 ± 0.03	
ph-PLN[b,c]	6.3 ± 0.1	0.45 ± 0.02	100 ± 5
R9C[b]	3.5 ± 0.1	0.39 ± 0.02	
ph-R9C	4.0 ± 0.1	0.41 ± 0.02	2.1 ± 0.25
R9L[b]	4.3 ± 0.1	0.40 ± 0.02	
ph-R9L	4.2 ± 0.2	0.41 ± 0.03	1.2 ± 0.04
R9H[b]	5.6 ± 0.1	0.90 ± 0.06	
ph-R9H	5.8 ± 0.2	0.84 ± 0.04	14 ± 3.0
R14del[b]	7.0 ± 0.2	0.74 ± 0.04	
ph-R14del	5.9 ± 0.2	0.72 ± 0.06	0.64 ± 0.20
R9C + wt[b]	5.1 ± 0.2	0.50 ± 0.04	
ph-(R9C + wt)	4.5 ± 0.1	0.47 ± 0.02	45 ± 2.9
R9H + wt	6.1 ± 0.6	0.86 ± 0.02	
ph-(R9H + wt)	4.8 ± 0.3	0.58 ± 0.07	44 ± 0.83
R9L + wt	5.3 ± 0.3	0.53 ± 0.07	
ph-(R9L + wt)	4.4 ± 0.2	0.46 ± 0.03	57 ± 3.6
R14del + wt[b]	5.3 ± 0.1	0.74 ± 0.02	
ph-(R14del + wt)	5.6 ± 0.2	0.59 ± 0.04	48 ± 7.1
PLN-SSS	7.4 ± 0.2	0.86 ± 0.04	98 ± 8.5
R9C-SSS	4.2 ± 0.2	0.47 ± 0.04	37 ± 3.9

[a] Percentage of phosphorylation compared with wild-type PLN of detergent-solubilized mutant PLN or wild-type/mutant mixtures of PLN.
[b] The kinetic data were taken from Ceholski *et al.* (18) and are shown for comparison.
[c] ph indicates that the PLN was treated with PKA prior to reconstitution.

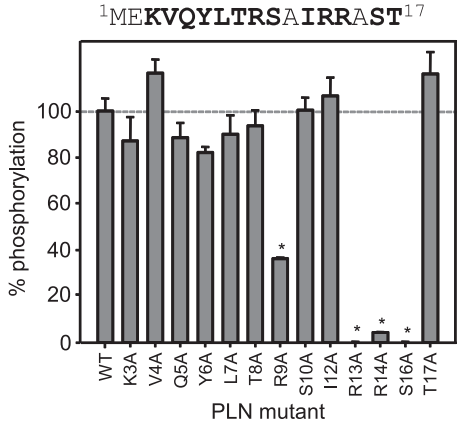

FIGURE 2. *Top panel,* primary sequence of PLN residues 1–17, with positions targeted for mutagenesis indicated (*bold letters*). *Bottom panel,* PKA-mediated phosphorylation of alanine mutants of these residues is shown as a percentage of wild-type PLN ± S.E. (100% = complete phosphorylation, *dashed line*) ($n \geq 4$). *Asterisks* indicate comparisons against wild type ($p < 0.01$).

For this reason, the goal of the present study was to mechanistically define the relationship between PLN mutation and the regulation of SERCA that underlies the development of DCM. To do this, we used reconstituted proteoliposomes containing SERCA and PLN under conditions that mimic native SR membrane (22, 25). Functional characterization of the proteoliposomes relied on measurements of the calcium-dependent ATPase activity of SERCA in the presence of wild-type or mutant PLN. R9C and R9L resulted in complete loss of function, R9H was indistinguishable from wild type, and R14del resulted in partial loss of function (Fig. 1, *A* and *B*, and Table 1). To mimic heterozygous conditions, mixtures of wild-type and mutant PLN (1:1 ratio) were reconstituted with SERCA. Because of increased hydrophobicity of the cytoplasmic domain of PLN, R9C, R9L, and R14del appeared to have a dominant negative effect on SERCA function (Table 1 and Ref. 18). Because R9H was a conservative mutation indistinguishable from wild-type PLN, it would not be considered a dominant negative regulator of SERCA.

Phosphorylation of PLN Mutants Implicated in Hereditary Cardiac Pathology—The cytoplasmic domain of PLN is the target of regulation via the β-adrenergic pathway, and disruption of this process would be expected to influence the development and progression of DCM. Although no known mutations affect the site of phosphorylation by PKA (Ser^{16}), Arg^{14} is part of the PKA recognition motif, and Arg^{9} is a more peripheral, upstream residue that may also be involved in recognition by PKA (31). Contrary to the location of these residues, R14del was initially reported to be phosphorylated, whereas R9C was reported to abrogate phosphorylation (9, 11). Therefore, our goal was to understand the relationship between disease-associated mutations and phosphoregulation of PLN. Under conditions that resulted in efficient phosphorylation of wild-type PLN (data not shown), we observed no detectable PKA-mediated phosphorylation of R9C, R9L, or R14del and minimal phosphorylation of R9H (Fig. 1*C*). This was confirmed with SERCA ATPase activity measurements, which revealed minimal changes in SERCA inhibition following PKA treatment of the PLN mutants (Table 1). This led us to consider whether the mutation of these particular residues (Arg^{9} and Arg^{14}) or the nature of the mutations (Cys, Leu, or His substitution or deletion) was the key determinant for the defect in phosphorylation.

To address this, we first tested the PKA-mediated phosphorylation of alanine mutants of residues Lys^{3} to Thr^{17} in the absence of SERCA (Fig. 2). Under conditions where wild-type PLN rapidly reached complete phosphorylation, most of the alanine substitutions between residues 3 and 17 resembled the native protein. However, three mutants (R9A, R13A, and R14A) exhibited clear defects in phosphorylation with S16A

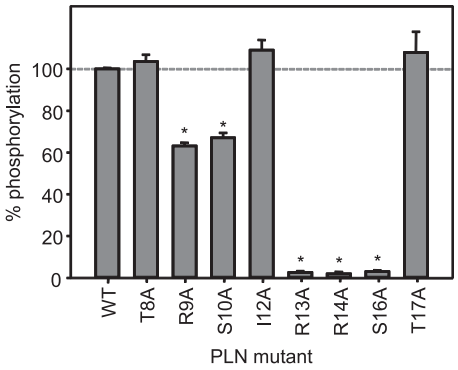

FIGURE 3. **PKA-mediated phosphorylation of PLN alanine mutants in proteoliposomes with SERCA.** Phosphorylation is shown as a percentage of wild-type PLN ± S.E. (100% = complete phosphorylation, *dashed line*) ($n \geq 4$). All phosphorylation values have been corrected for PLN content of the proteoliposomes. *Asterisks* indicate comparisons against wild type ($p < 0.01$).

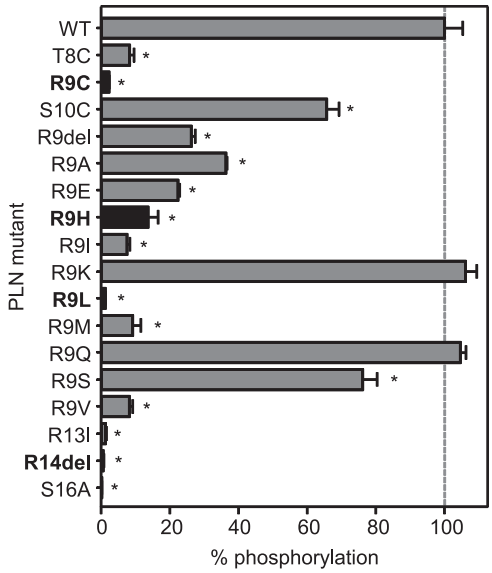

FIGURE 4. **PKA-mediated phosphorylation of disease-mimicking PLN mutants.** Phosphorylation is shown as a percentage of wild-type PLN ± S.E. (100% = complete phosphorylation, *dashed line*) ($n \geq 4$). Disease-causing mutations are labeled in *bold type* and shown with *black bars*. *Asterisks* indicate comparisons against wild type ($p < 0.01$).

serving as a negative control. The results for Arg^{13} and Arg^{14} were anticipated given their placement in the PKA recognition motif and prior characterization by mutagenesis (32). The result for Arg^{9} of PLN was unexpected, given that it was not previously reported to be a determinant for PKA-mediated phosphorylation (17).

PLN in the absence of SERCA allowed unhindered interaction with PKA for optimal phosphorylation, yet this did not take into account the SERCA-PLN interaction that normally occurs in cardiac SR. To examine this, proteoliposomes containing SERCA in the presence of wild-type or mutant PLN were phosphorylated by PKA. To distinguish between SERCA-specific effects on PLN phosphorylation *versus* molecular crowding that could limit the accessibility of PKA, the reconstitution method was altered to incorporate a higher lipid to protein ratio in the proteoliposomes (25). Under conditions where wild-type PLN rapidly reached complete phosphorylation, we again observed significant decreases in the phosphorylation of R9A, R13A, and R14A (Fig. 3). Surprisingly, the S10A mutation now exhibited reduced phosphorylation (67 ± 4.2% of wild type) comparable with the reduction observed for the R9A mutant (63 ± 2.8% of wild type). The reduced phosphorylation of S10A only occurred in the presence of SERCA, indicating that this residue may be important for PKA recognition and binding of SERCA-bound PLN. It should be noted that this reduced level of phosphorylation corresponded to more than one molecule of PLN per molecule of SERCA.

Mimicking Disease-associated Mutations in PLN—So far, the R9C, R9H, R9L, and R14del mutations have only been found in heterozygous individuals, where they exert a dominant negative effect on calcium reuptake. In particular, the R9C mutant was reported to trap PKA and block phosphorylation of wild-type PLN (11). The dominant negative effect of R9C on PKA-mediated phosphorylation prompted us to investigate equimolar mixtures of mutant and wild-type PLN in our phosphorylation assays (Table 1). To allow for the formation of a trapped, inactive complex with PKA, the assays were performed with or without preincubation of PKA with the R9C, R9L, R9H, or R14del mutants. Under these conditions, none of the mutants sequestered PKA and prevented the phosphorylation of wild-type PLN. This was supported by SERCA ATPase activity measurements, where the phosphorylation of wild-type PLN had the expected effects on heterozygous mixtures with the mutants (R9C, R9L, R9H, and R14del; Table 1). Our conclusion was that a simple interaction between the PLN mutant and PKA did not result in trapping, suggesting that something more complicated may be occurring in DCM. SERCA, PLN, and PKA are part of a larger signaling complex that includes protein kinase A-anchoring protein AKAP18δ (33), as well as additional regulatory components. It is reasonable to expect that one or more of these interactions may be perturbed in R9C-mediated DCM.

Nonetheless, the lack of phosphorylation of R9C, R9H, R9L, and R14del mutants by PKA prompted us to further investigate by generating a series of amino acid substitutions of and around Arg^{9} and Arg^{14}. The Arg^{14} deletion mutant shortens the N-terminal cytoplasmic domain of PLN and changes the PKA recognition motif from Arg^{13}-Arg^{14}-Ala^{15}-Ser^{16} to Ile^{12}-Arg^{13}-Ala^{15}-Ser^{16} (Fig. 2). This change interferes with SERCA and PKA interactions necessary for the proper regulation of calcium reuptake. We have already shown that R14del cannot be phosphorylated by PKA and that R13A and R14A recapitulate this behavior. To confirm these observations, we mutated Arg^{13} to isoleucine (R13I) to mimic the amino acid sequence change that results from deletion of Arg^{14} (the sequence became Ile^{13}-Arg^{14}-Ala^{15}-Ser^{16}) without shortening the cytoplasmic domain of PLN. Like R14del, we found that R13I could not be phosphorylated by PKA (Fig. 4). The combined results for R14del, R13A, R14A, and R13I indicated that any change to the PKA recognition motif of PLN would be expected to eliminate PLN phosphorylation as a means of regulating SERCA function.

We next investigated the physicochemical properties of R9C, R9H, and R9L that contribute to PLN dysregulation and DCM. The mutants tested included R9A, R9C, R9E (charge reversal), R9del (deletion of Arg^{9}), R9S (isosteric to R9C), R9K and R9H (conservative substitutions), R9Q (removal of charge), and R9L,

R9V, R9I, and R9M (hydrophobic substitutions). All mutations of Arg^9 except for R9K and R9Q reduced phosphorylation by PKA (Fig. 4), whereas R9C, R9H, and all hydrophobic substitutions (R9L, R9V, R9I, and R9M) completely or nearly abolished phosphorylation. Surprisingly, the hydrophobic substitutions were the most effective mimics of the phosphorylation defects associated with R9C and R9L, mirroring the trend observed for the functional defects associated with these mutants (18). Additionally, R9H was found to cause a severe defect in phosphorylation, consistent with the potential linkage of this mutation to heart failure (12). Although histidine is a conservative substitution for arginine, the aromatic side chain likely makes it a poor substrate for PKA phosphorylation. We next investigated the positioning of the cysteine substitution at Arg^9. We generated isosteric mutations of nearby residues Thr^8 and Ser^{10} to cysteine (T8C and S10C). Neither mutant exactly mimicked R9C, yet T8C clearly resulted in a strong defect in phosphorylation. We concluded that Arg^9 is important for the recognition of PLN by PKA and that a hydrophobic mutation in this region of PLN is particularly detrimental for phosphorylation by PKA.

Arg^9 of PLN and Complementary Residues of PKA—Previous studies have suggested that PKA prefers peptide substrates with a basic residue upstream of the recognition motif at the P-6, P-7, or P-8 position (31, 34), although the role of such distal residues in natural substrates like PLN has been less apparent. In model substrates, the upstream arginine is not required for phosphorylation, yet it plays a role in peptide positioning in the active site of PKA and increases the efficiency of phosphorylation. Herein, mutagenesis revealed that Arg^9 at P-7 of PLN appeared to fit this notion, where removal of the arginine side chain (R9A) decreased the efficiency of PLN phosphorylation, and substitution of particular side chains (hydrophobic substitutions) completely abolished phosphorylation (Fig. 4). The structure of the catalytic subunit of PKA bound to a cytoplasmic peptide of PLN has been determined (35), and it identifies two acidic residues in PKA (Glu^{203} and Asp^{241}) that interact with Arg^9 of PLN (Fig. 5). To assess the importance of these residues, we produced recombinant bovine catalytic subunit of wild-type PKA, as well as Glu^{203} to Ala (E203A) and Asp^{241} to Ala (D241A) mutants of PKA. The activity of these PKA variants was confirmed using kemptide (sequence LRRASLG) (36), an ideal substrate for PKA based on the phosphorylation site of liver pyruvate kinase (Table 2).

Phosphorylation of PLN by Recombinant PKA—Although model peptides are a facile system for studying phosphorylation, full-length, membrane-associated PLN is the natural substrate for PKA. However, the disease-associated Arg^9 mutants of PLN could not be phosphorylated over the time frame of our experiments. For this reason, the R9S mutant was chosen as a surrogate. R9S is isosteric to R9C, yet it resulted in sufficient phosphorylation for the study of PKA mutants (Fig. 4). Under the experimental conditions, recombinant wild-type PKA phosphorylated wild-type PLN with a half-time of ~7.5 min and an initial rate of 12.2 μmol min^{-1} (Fig. 6*A*). Phosphorylation of R9S PLN with recombinant wild-type PKA resulted in a lower initial rate, and the time-dependent phosphorylation saturated but never reached complete phosphorylation. A similar trend occurred for the E203A mutant of PKA with both wild-type and R9S PLN (Fig. 6*B*). In fact, the progress curves for these three enzyme-substrate pairs (wild-type PKA with R9S PLN, E203A PKA with wild-type PLN, and E203A PKA with R9S PLN) were very similar to one another and did not reach complete phosphorylation. This suggested a common underlying effect on phosphorylation. Lastly, we tested the D241A mutant of PKA, which had a more severe effect on the phosphorylation of PLN (Fig. 6*C*). The data are consistent with interactions

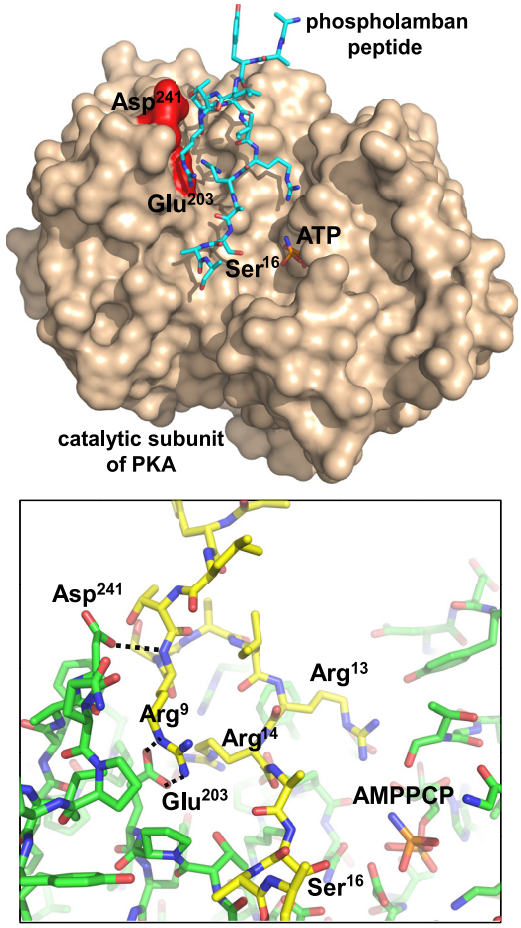

FIGURE 5. *Top panel*, molecular model for the interaction between PKA (surface representation) and PLN (residues Lys^3–Thr^{17}; stick representation) based on structures of PKA bound to peptides (Protein Data Bank entries 1JLU, 1JBP, and 3O7L). Negatively charged residues in PKA are shown in *red* (Glu^{203} and Asp^{241}). The phosphorylated Ser^{16} of PLN and ATP are labeled. *Bottom panel*, a detailed view of the PKA active site containing PLN reveals that Arg^9 of PLN forms electrostatic interactions with Glu^{203} and Asp^{241} of PKA. The backbones of PKA residues are shown in *green*, and the backbones of PLN residues are shown in *yellow*. Arg^9, Arg^{13}, Arg^{14}, and Ser^{16} of PLN, Glu^{203} and Asp^{241} of PKA, and AMP-PCP are labeled.

TABLE 2
Steady-state kinetic parameters for PKA mutants

Kinetic parameters	PLN peptide		
	Kemptide	Wild type	R9C
Wild-type PKA			
K_m (μM)	13.8 ± 0.6	6.8 ± 2.1	11.0 ± 2.6
k_{cat}/K_m (μM^{-1} s^{-1})	2.06 ± 0.18	5.43 ± 0.73	0.80 ± 0.13
E203A PKA			
K_m (μM)	81.0 ± 5.9	70.1 ± 5.4	69.0 ± 11.4
k_{cat}/K_m (μM^{-1} s^{-1})	0.60 ± 0.16	0.65 ± 0.19	0.11 ± 0.04
D241A PKA			
K_m (μM)	17.2 ± 2.1	6.84 ± 2.4	9.6 ± 4.1
k_{cat}/K_m (μM^{-1} s^{-1})	0.23 ± 0.02	0.79 ± 0.09	0.12 ± 0.02

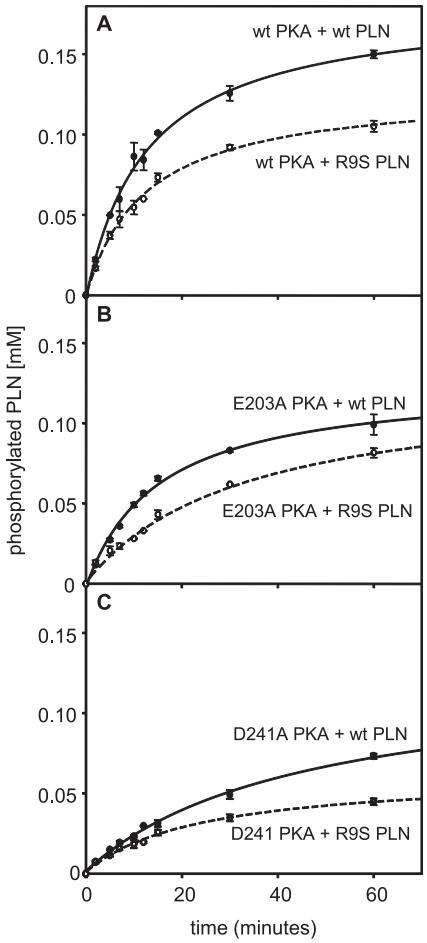

FIGURE 6. **Time-dependent phosphorylation of wild-type (●, *solid line*) or R9S (○, *dashed line*) PLN ± S.E. by recombinant wild-type (*A*), E203A (*B*), or D241A (*C*) PKA.** Concentration of phosphorylated PLN (mM) is shown as a function of time (minutes) ($n \geq 3$).

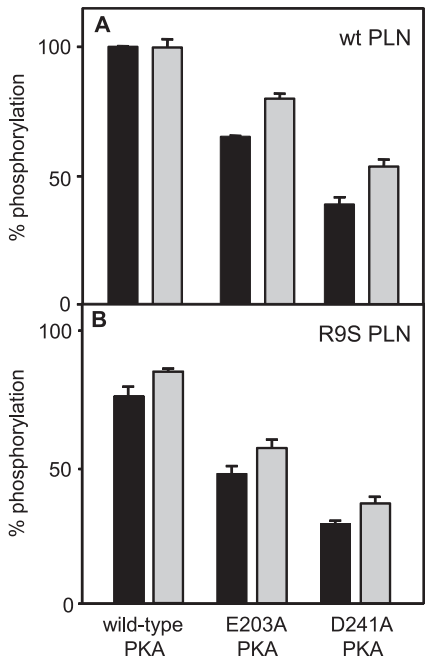

FIGURE 7. **Phosphorylation of wild-type PLN (*A*) or R9S PLN (*B*) ± S.E. by recombinant wild-type, E203A, or D241A PKA.** Phosphorylation of PLN (*black bars*) and after an additional double aliquot of PKA (*gray bars*) are compared ($n \geq 3$).

between Glu^{203} and the side chain of Arg^{9} and Asp^{241} and the backbone amide of Arg^{9} (Fig. 5), both of which are required for positioning of the substrate for efficient phosphorylation.

The progress curves for the three enzyme-substrate pairs described above never reached complete phosphorylation, consistent with either enzyme inactivation or substrate depletion. Enzyme inactivation, perhaps by denaturation or product inhibition, seemed unlikely because the enzyme was limiting in the reactions. Nevertheless, a simple test for enzyme inactivation was to incubate the three PKA variants (wild type, E203A, and D241A) with wild-type PLN until saturation was reached, followed by the addition of fresh enzyme to test whether phosphorylation could proceed. We found that the addition of enzyme did not result in complete phosphorylation of wild-type PLN by the PKA mutants (Fig. 7*A*), indicating that enzyme inactivation was not the cause of this behavior. This same result was observed with R9S PLN, where the addition of fresh PKA (wild type or mutant) was unable to complete R9S phosphorylation (Fig. 7*B*). We then wondered how the substrate might change as a function of time in the progress curves. Because the substrate, wild-type or R9S PLN, was identical for all three PKA variants, it seemed improbable that true substrate depletion was occurring. Instead, it seemed more likely that the accessibility of the substrate to PKA changed as product accumulated in the phosphorylation reactions. The simplest way to envision how this might occur was to invoke phosphorylation in the context of the PLN pentamer (37). To take this into account, we replotted the progress curves for wild-type PKA and R9S PLN and E203A PKA and wild-type PLN as a function of the number of phosphorylated monomeric equivalents (Fig. 8*A*). For mutation of either PLN (Arg^{9}) or PKA (Glu^{203}), the progress curves stalled after the phosphorylation of two to three monomers per PLN pentamer. This led to the hypothesis that these residues of PLN and PKA function, at least in part, to recognize a non-phosphorylated monomer in the context of a partially phosphorylated pentamer.

If this hypothesis was correct, reducing the oligomeric state of PLN should increase the level of phosphorylation. For this, we returned to the disease-associated R9C mutant, which could not be phosphorylated by PKA in our assays and thus provided a rigorous test for our hypothesis. A full-length monomeric form of R9C (R9C-SSS) and an R9C cytoplasmic peptide ($R9C_{1-20}$, amino acids 1–20 of PLN) were both tested for their ability to be phosphorylated by PKA. The monomeric form of PLN was generated by replacing the three transmembrane cysteine residues (Cys^{36}, Cys^{41}, and Cys^{46}) with serine. The PLN-SSS and R9C-SSS mutants were entirely monomeric by SDS-PAGE (Fig. 8*B*), and they possessed inhibitory properties comparable with wild-type and R9C PLN, respectively (Table 1). As might be expected, R9C-SSS increased phosphorylation ~22-fold compared with R9C (to ~37% phosphorylation level of wild type), whereas $R9C_{1-20}$ increased phosphorylation 45-fold compared with R9C (to ~84% phosphorylation level of wild type) (Fig. 8*C* and Table 2). The increase in phosphorylation of the monomeric forms of R9C indicated that the quaternary structure of the pentamer is a limiting factor in the phosphorylation of individual subunits. Thus, the specific rec-

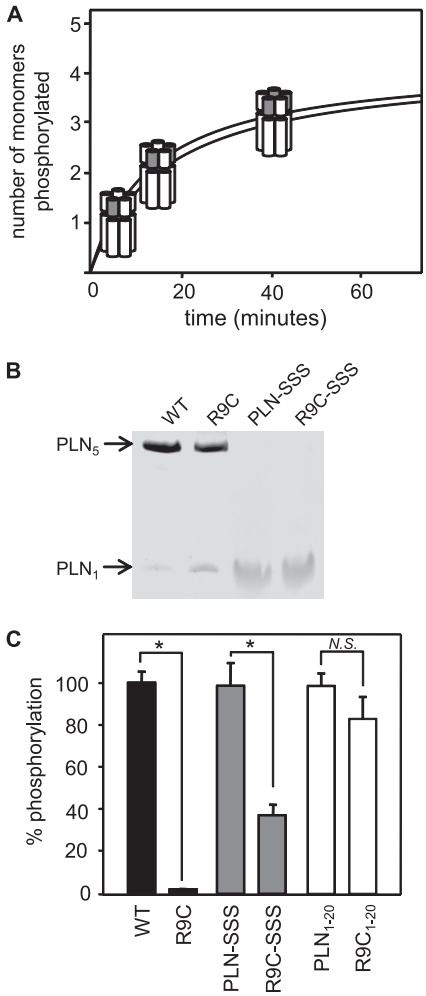

FIGURE 8. *A*, time-dependent phosphorylation progress curves of wild-type PKA and R9S PLN and E203A PKA and wild-type PLN were replotted as a function of phosphorylated monomeric equivalent units. Phosphorylation stalled when two or three monomers in a pentamer were phosphorylated. *B*, SDS-PAGE of wild-type, R9C, PLN-SSS, and R9C-SSS PLN (5 μg/lane). Pentameric (PLN_5) and monomeric (PLN_1) PLN are indicated with *arrows*. *C*, PKA-mediated phosphorylation of wild-type PLN *versus* R9C PLN, monomeric PLN-SSS *versus* R9C-SSS, and cytoplasmic peptide PLN_{1-20} *versus* $R9C_{1-20}$ ($n \geq 3$; % phosphorylation ± S.E.). *Asterisks* indicate comparisons against each respective wild-type construct ($p < 0.01$). *N.S.*, not significant.

ognition of Arg^9 by PKA helps to overcome this, reminiscent of the role of the pentamer in PLN dephosphorylation (37). In addition, the R9C monomer did not reach wild-type levels of phosphorylation, indicating that Arg^9 of PLN is important for the efficient phosphorylation of this longer, natural substrate of PKA.

DISCUSSION

Thus far, four mutations linked to heart disease have been identified in the cytoplasmic domain of PLN (9, 11, 12, 38). The first to be identified was an R9C mutant, followed by R14del and newly identified R9H and R9L. Deletion of Arg^{14} was found in two families with autosomal dominant DCM resulting in death at middle age (9, 39), as well as another small family with late onset mild DCM (38). A heterozygous mouse model generated for this mutant suggested it was a superinhibitor of SERCA that was only partially reversible by PKA-mediated phosphorylation (9). By comparison, the R9C mutant results in multiple changes to PLN function. A heterozygous mouse model suggested that R9C is a loss of function form of PLN that also traps PKA and prevents the phosphorylation of other cellular targets including wild-type PLN (11). The effects of R9H and R9L on SERCA inhibition have been characterized (18), but their consequences on phosphorylation have yet to be examined. Given the link of R9C and R14del to PLN phosphorylation, we systematically examined the residues surrounding the phosphorylation site of PLN for their disease relevance. We wished to examine the aberrant interactions involving only PLN-SERCA and PLN-PKA, both of which would be considered initiating events in the development of DCM. At the cellular level, these initiating events could be distinct from observations made at later stages of disease development, where many affected processes can ultimately contribute to the observed suppression of SERCA function.

Mechanism of Disease-causing Mutations of PLN—First considering R14del, it was initially reported to be a partial inhibitor of SERCA under homozygous conditions and a superinhibitor under heterozygous conditions in HEK-293 cells (9). It was also observed that R14del may be phosphorylated, despite the change to the PKA recognition motif. A later study in mouse models revealed that under homozygous conditions, R14del was misdirected to the plasma membrane where it altered the activity of the sodium pump (40). In this latter study, R14del did not inhibit SERCA and was only weakly phosphorylated. However, only heterozygous R14del patients have been identified, and it has been shown that R14del is retained in the SR under heterozygous conditions (9). This suggests that the presence of both mutant and wild-type PLN underlies the development of DCM, perhaps via the reported superinhibition of SERCA. To investigate this, we isolated SERCA and R14del from all other cellular effectors and found it to be a partial inhibitor of SERCA (slight loss of function mutant) in both the absence and presence of wild-type PLN (18). We also observed that R14del could not be phosphorylated by PKA. Putting this in terms of initial stages of calcium dysregulation, R14del would result in partial inhibition of SERCA and lack of β-adrenergic control by phosphorylation. This initial chronic inhibition of SERCA could lead to the development of other cellular sequelae, such as SERCA down-regulation (29, 30) or changes in the SUMOylation of SERCA (41).

By comparison with R14del, the R9C mutant resulted in multiple changes to PLN function, including the purported trapping of PKA. Given that a cysteine residue replaced Arg^9 of PLN, we immediately considered the aberrant chemistry of a free sulfhydryl as the culprit for disease (42). However, examination of the structure of the PKA substrate-binding pocket revealed no obvious mechanism for the formation of a trapped complex (35). Further investigation revealed that a hydrophobic substitution at this position was enough to completely mimic R9C, and we anticipated that mutations like R9L might eventually be found in the human population (18). Of course, we now know that Arg^9 is a hot spot for disease-associated mutations, as can be seen with the recent identification of R9H and R9L in heart disease patients (12). Perhaps this is not surprising, because PKA prefers an arginine six to eight residues upstream of the recognition motif (31, 43), and dynamic phos-

phorylation of PLN is critical for normal cardiac function (44–46). The available data suggest that the free and PKA-bound conformations of PLN are distinct (35) and that interconversion is more efficient with Arg^9 present. One can then speculate that hydrophobic substitution of Arg^9 is detrimental because it alters interactions necessary for the free or PKA-bound conformations of PLN (35, 47, 48). From the standpoint of establishing prediction models for human heart failure, any of the hydrophobic substitutions identified herein (such as T8C, R9I, R9M, R9V, and R13I) would be expected to mimic the disease development seen for R9C and R9L. One interesting mutant to note was R9H, recently identified in a Brazilian cohort of heart failure patients (12). The R9H mutation was found in a single patient with idiopathic DCM and was considered a low penetrant allele because several family members had the PLN mutation in the absence of disease. However, R9H resembles the disease-associated R14del mutation in that it is a functional inhibitor of SERCA (18), which cannot be phosphorylated by PKA (Fig. 4). As a result, R9H would be unresponsive to β-adrenergic stimulation, leading to constitutive inhibition of SERCA. Although this by itself may not be causative in disease, we anticipate that individuals harboring the R9H mutation would be predisposed to heart failure.

Arg^9 Is Important for Proper Positioning of PLN in PKA Active Site—Arginine residues in the cytoplasmic domain of PLN appear to be hot spots for disease-associated mutations. At first glance this suggests a common underlying disease mechanism, although two of the mutants are partly functional (R9H and R14del), and two are nonfunctional (R9C and R9L). Although the hereditary PLN mutations do not have a common effect on the functional state of PLN (*i.e.* SERCA inhibition), all of the mutants appear to implicate PKA in disease (9, 11). As part of the PKA recognition motif, deletion of Arg^{14} was expected to have a major impact on PLN phosphorylation (Fig. 4 and Refs. 9 and 32). In addition, it has been known for some time that PKA prefers model substrates with an arginine residue N-terminal to the recognition motif (31). The structure of PKA with an inhibitor (protein kinase inhibitor, PKI) shows that an upstream arginine interacts with Glu^{203}, which is part of the peptide positioning loop of PKA (31, 49). As a natural substrate, Arg^9 of PLN fits this notion of an upstream arginine, and the recent crystal structure of the PLN cytoplasmic domain bound to PKA clearly revealed interactions of Arg^9 with the peptide positioning loop of PKA (Fig. 5 and Ref. 35). As a natural PKA substrate, Arg^9 of PLN appears to be positioned by Glu^{203} and Asp^{241} of PKA, yet the functional implications of these interactions remain poorly elucidated. Herein we have shown that Arg^9 and Arg^{14} of PLN and Glu^{203} and Asp^{241} of PKA are essential for phosphorylation, providing a possible shared mechanism for the disease-associated mutations. The presence of Arg^9 offers the advantage of increased substrate affinity and efficiency of phosphorylation (Table 2). If Arg^9, Glu^{203}, or Asp^{241} is mutated, PKA can no longer discriminate between PLN and a model substrate such as kemptide. As for the role of each residue in the proper positioning of PLN in the active site of PKA, Arg^9 contributes to both binding affinity and catalytic efficiency, Glu^{203} makes a larger contribution to binding affinity, and Asp^{241} influences catalytic efficiency.

Role of Arg^9 of PLN in Efficient Phosphorylation of PLN Pentamer—Mutation of Arg^9 of PLN or Glu^{203} or Asp^{241} of PKA resulted in a plateau in phosphorylation at ~60% of total PLN (Fig. 6). The prospect of enzyme inactivation was eliminated when the addition of extra PKA failed to fully phosphorylate PLN (Fig. 7), and it was equally unlikely that substrate depletion was responsible. Instead, our results indicated that partial phosphorylation correlated with the oligomeric state of PLN. Disrupting the ability of PLN to form a pentamer, either by mutation (R9C-SSS PLN) or the use of a cytoplasmic peptide ($R9C_{1-20}$), markedly increased phosphorylation at Ser^{16} (Fig. 8*C*). Because PLN phosphorylation occurs randomly, with each monomer within a pentamer having an equal chance at becoming phosphorylated (37), phosphorylation appeared to stall after two or three monomers within the pentamer were phosphorylated. Thus, we concluded that Arg^9 of PLN, along with Glu^{203} and Asp^{241} of PKA, are required for the phosphorylation of a monomer within the context of a partially phosphorylated pentamer. This observation may provide an explanation for the PKA trapping reported for the R9C mutation in lethal DCM (11).

It has been reported that the conformational dynamics of PLN are an important determinant for PKA-mediated phosphorylation (50) and that PKA recognizes substrates by conformational selection (35). Herein we find that Arg^9 plays a dual role: it increases the efficiency of phosphorylation of a PLN monomer, and it allows for recognition of a monomer within the context of the PLN pentamer. Although PLN is a dynamic molecule, it also possesses a well defined structure that is distinct from that in the PKA-bound state (35, 48). Thus, in the selection of an appropriate substrate conformation by PKA, the presence of Arg^9 in PLN must offer an advantage for the recognition of a suitably structured substrate. The absence of Arg^9 in disease-causing mutants of PLN (such as R9C, R9H, and R9L) could alter the conformational selection by PKA, thereby creating a kinetic trap for PKA and affecting the phosphorylation of other cellular targets. Additionally, it is becoming clear that hydrophobic substitution of Arg^9 creates multiple defects in PLN function, including loss of phosphorylation and an abnormal interaction with PKA, as well as loss of inhibitory function and a dominant negative interaction with SERCA (18). In the case of R9C, this could be further exacerbated by disulfide bond formation between PLN monomers (42). Because the associated defects in calcium homeostasis appear to be causative in heart failure, arginine residues in the cytoplasmic domain of PLN should be considered functional hot spots for hereditary mutations.

Acknowledgments—We thank Leah Stables, Tamara Skene-Arnold, Phuwadet Pasarj, Craig Markin, Leo Spyracopoulos, Ghazaleh Ashrafi, and Michael Martyna for valuable assistance.

REFERENCES

1. Tada, M., Kirchberger, M. A., and Katz, A. M. (1976) Regulation of calcium transport in cardiac sarcoplasmic reticulum by cyclic AMP-dependent protein kinase. *Recent Adv. Stud. Cardiac Struct. Metab.* **9,** 225–239
2. Morgan, J. P. (1991) Abnormal intracellular modulation of calcium as a major cause of cardiac contractile dysfunction. *N. Engl. J. Med.* **325,**

625–632
3. Simmerman, H. K., Collins, J. H., Theibert, J. L., Wegener, A. D., and Jones, L. R. (1986) Sequence analysis of phospholamban. Identification of phosphorylation sites and two major structural domains. *J. Biol. Chem.* **261,** 13333–13341
4. Schmidt, A. G., Edes, I., and Kranias, E. G. (2001) Phospholamban. A promising therapeutic target in heart failure? *Cardiovasc. Drugs Ther.* **15,** 387–396
5. Grünig, E., Tasman, J. A., Kücherer, H., Franz, W., Kübler, W., and Katus, H. A. (1998) Frequency and phenotypes of familial dilated cardiomyopathy. *J. Am. Coll. Cardiol.* **31,** 186–194
6. Brittsan, A. G., and Kranias, E. G. (2000) Phospholamban and cardiac contractile function. *J. Mol. Cell Cardiol.* **32,** 2131–2139
7. Luo, W., Wolska, B. M., Grupp, I. L., Harrer, J. M., Haghighi, K., Ferguson, D. G., Slack, J. P., Grupp, G., Doetschman, T., Solaro, R. J., and Kranias, E. G. (1996) Phospholamban gene dosage effects in the mammalian heart. *Circ. Res.* **78,** 839–847
8. Frank, K. F., Bölck, B., Brixius, K., Kranias, E. G., and Schwinger, R. H. (2002) Modulation of SERCA. Implications for the failing human heart. *Basic Res. Cardiol.* **97,** I72–I78
9. Haghighi, K., Kolokathis, F., Gramolini, A. O., Waggoner, J. R., Pater, L., Lynch, R. A., Fan, G. C., Tsiapras, D., Parekh, R. R., Dorn, G. W., 2nd, MacLennan, D. H., Kremastinos, D. T., and Kranias, E. G. (2006) A mutation in the human phospholamban gene, deleting arginine 14, results in lethal, hereditary cardiomyopathy. *Proc. Natl. Acad. Sci. U.S.A.* **103,** 1388–1393
10. Haghighi, K., Kolokathis, F., Pater, L., Lynch, R. A., Asahi, M., Gramolini, A. O., Fan, G. C., Tsiapras, D., Hahn, H. S., Adamopoulos, S., Liggett, S. B., Dorn, G. W., 2nd, MacLennan, D. H., Kremastinos, D. T., and Kranias, E. G. (2003) Human phospholamban null results in lethal dilated cardiomyopathy revealing a critical difference between mouse and human. *J. Clin. Invest.* **111,** 869–876
11. Schmitt, J. P., Kamisago, M., Asahi, M., Li, G. H., Ahmad, F., Mende, U., Kranias, E. G., MacLennan, D. H., Seidman, J. G., and Seidman, C. E. (2003) Dilated cardiomyopathy and heart failure caused by a mutation in phospholamban. *Science* **299,** 1410–1413
12. Medeiros, A., Biagi, D. G., Sobreira, T. J., de Oliveira, P. S., Negrão, C. E., Mansur, A. J., Krieger, J. E., Brum, P. C., and Pereira, A. C. (2011) Mutations in the human phospholamban gene in patients with heart failure. *Am. Heart J.* **162,** 1088–1095
13. Haghighi, K., Schmidt, A. G., Hoit, B. D., Brittsan, A. G., Yatani, A., Lester, J. W., Zhai, J., Kimura, Y., Dorn, G. W., 2nd, MacLennan, D. H., and Kranias, E. G. (2001) Superinhibition of sarcoplasmic reticulum function by phospholamban induces cardiac contractile failure. *J. Biol. Chem.* **276,** 24145–24152
14. Zhai, J., Schmidt, A. G., Hoit, B. D., Kimura, Y., MacLennan, D. H., and Kranias, E. G. (2000) Cardiac-specific overexpression of a superinhibitory pentameric phospholamban mutant enhances inhibition of cardiac function *in vivo*. *J. Biol. Chem.* **275,** 10538–10544
15. Zvaritch, E., Backx, P. H., Jirik, F., Kimura, Y., de Leon, S., Schmidt, A. G., Hoit, B. D., Lester, J. W., Kranias, E. G., and MacLennan, D. H. (2000) The transgenic expression of highly inhibitory monomeric forms of phospholamban in mouse heart impairs cardiac contractility. *J. Biol. Chem.* **275,** 14985–14991
16. Kimura, Y., Kurzydlowski, K., Tada, M., and MacLennan, D. H. (1996) Phospholamban regulates the Ca^{2+}-ATPase through intramembrane interactions. *J. Biol. Chem.* **271,** 21726–21731
17. Fujii, J., Maruyama, K., Tada, M., and MacLennan, D. H. (1989) Expression and site-specific mutagenesis of phospholamban. Studies of residues involved in phosphorylation and pentamer formation. *J. Biol. Chem.* **264,** 12950–12955
18. Ceholski, D. K., Trieber, C. A., and Young, H. S. (2012) Hydrophobic imbalance in the cytoplasmic domain of phospholamban is a determinant for lethal dilated cardiomyopathy. *J. Biol. Chem.* **287,** 16521–16529
19. Eletr, S., and Inesi, G. (1972) Phospholipid orientation in sarcoplasmic membranes. Spin-label ESR and proton MNR studies. *Biochim. Biophys. Acta* **282,** 174–179
20. Stokes, D. L., and Green, N. M. (1990) Three-dimensional crystals of CaATPase from sarcoplasmic reticulum. Symmetry and molecular packing. *Biophys. J.* **57,** 1–14
21. Douglas, J. L., Trieber, C. A., Afara, M., and Young, H. S. (2005) Rapid, high-yield expression and purification of Ca^{2+}-ATPase regulatory proteins for high-resolution structural studies. *Protein Expr. Purif.* **40,** 118–125
22. Trieber, C. A., Douglas, J. L., Afara, M., and Young, H. S. (2005) The effects of mutation on the regulatory properties of phospholamban in co-reconstituted membranes. *Biochemistry* **44,** 3289–3297
23. Young, H. S., Reddy, L. G., Jones, L. R., and Stokes, D. L. (1998) Co-reconstitution and co-crystallization of phospholamban and Ca^{2+}-ATPase. *Ann. N.Y. Acad. Sci.* **853,** 103–115
24. Warren, G. B., Toon, P. A., Birdsall, N. J., Lee, A. G., and Metcalfe, J. C. (1974) Reconstitution of a calcium pump using defined membrane components. *Proc. Natl. Acad. Sci. U.S.A.* **71,** 622–626
25. Young, H. S., Rigaud, J. L., Lacapère, J. J., Reddy, L. G., and Stokes, D. L. (1997) How to make tubular crystals by reconstitution of detergent-solubilized Ca^{2+}-ATPase. *Biophys. J.* **72,** 2545–2558
26. Young, H. S., Jones, L. R., and Stokes, D. L. (2001) Locating phospholamban in co-crystals with Ca^{2+}-ATPase by cryoelectron microscopy. *Biophys. J.* **81,** 884–894
27. Studier, F. W. (2005) Protein production by auto-induction in high density shaking cultures. *Protein Expr. Purif.* **41,** 207–234
28. Hastie, C. J., McLauchlan, H. J., and Cohen, P. (2006) Assay of protein kinases using radiolabeled ATP. A protocol. *Nat. Protoc.* **1,** 968–971
29. Meyer, M., Schillinger, W., Pieske, B., Holubarsch, C., Heilmann, C., Posival, H., Kuwajima, G., Mikoshiba, K., Just, H., and Hasenfuss, G. (1995) Alterations of sarcoplasmic reticulum proteins in failing human dilated cardiomyopathy. *Circulation* **92,** 778–784
30. Hasenfuss, G., Reinecke, H., Studer, R., Meyer, M., Pieske, B., Holtz, J., Holubarsch, C., Posival, H., Just, H., and Drexler, H. (1994) Relation between myocardial function and expression of sarcoplasmic reticulum Ca^{2+}-ATPase in failing and nonfailing human myocardium. *Circ. Res.* **75,** 434–442
31. Moore, M. J., Adams, J. A., and Taylor, S. S. (2003) Structural basis for peptide binding in protein kinase A. Role of glutamic acid 203 and tyrosine 204 in the peptide-positioning loop. *J. Biol. Chem.* **278,** 10613–10618
32. Toyofuku, T., Kurzydlowski, K., Tada, M., and MacLennan, D. H. (1994) Amino acids Glu^2 to Ile^{18} in the cytoplasmic domain of phospholamban are essential for functional association with the Ca^{2+}-ATPase of sarcoplasmic reticulum. *J. Biol. Chem.* **269,** 3088–3094
33. Lygren, B., Carlson, C. R., Santamaria, K., Lissandron, V., McSorley, T., Litzenberg, J., Lorenz, D., Wiesner, B., Rosenthal, W., Zaccolo, M., Taskén, K., and Klussmann, E. (2007) AKAP complex regulates Ca^{2+} re-uptake into heart sarcoplasmic reticulum. *EMBO Rep.* **8,** 1061–1067
34. Neuberger, G., Schneider, G., and Eisenhaber, F. (2007) pkaPS. Prediction of protein kinase A phosphorylation sites with the simplified kinase-substrate binding model. *Biol. Direct* **2,** 1
35. Masterson, L. R., Cheng, C., Yu, T., Tonelli, M., Kornev, A., Taylor, S. S., and Veglia, G. (2010) Dynamics connect substrate recognition to catalysis in protein kinase A. *Nat. Chem. Biol.* **6,** 821–828
36. Kemp, B. E., Graves, D. J., Benjamini, E., and Krebs, E. G. (1977) Role of multiple basic residues in determining the substrate specificity of cyclic AMP-dependent protein kinase. *J. Biol. Chem.* **252,** 4888–4894
37. Li, C. F., Wang, J. H., and Colyer, J. (1990) Immunological detection of phospholamban phosphorylation states facilitates the description of the mechanism of phosphorylation and dephosphorylation. *Biochemistry* **29,** 4535–4540
38. DeWitt, M. M., MacLeod, H. M., Soliven, B., and McNally, E. M. (2006) Phospholamban R14 deletion results in late-onset, mild, hereditary dilated cardiomyopathy. *J. Am. Coll. Cardiol.* **48,** 1396–1398
39. Posch, M. G., Perrot, A., Geier, C., Boldt, L. H., Schmidt, G., Lehmkuhl, H. B., Hetzer, R., Dietz, R., Gutberlet, M., Haverkamp, W., and Ozcelik, C. (2009) Genetic deletion of arginine 14 in phospholamban causes dilated cardiomyopathy with attenuated electrocardiographic R amplitudes. *Heart Rhythm* **6,** 480–486
40. Haghighi, K., Pritchard, T., Bossuyt, J., Waggoner, J. R., Yuan, Q., Fan, G. C., Osinska, H., Anjak, A., Rubinstein, J., Robbins, J., Bers, D. M., and

Kranias, E. G. (2012) The human phospholamban Arg14-deletion mutant localizes to plasma membrane and interacts with the Na/K-ATPase. *J. Mol. Cell. Cardiol.* **52,** 773–782
41. Kho, C., Lee, A., Jeong, D., Oh, J. G., Chaanine, A. H., Kizana, E., Park, W. J., and Hajjar, R. J. (2011) SUMO1-dependent modulation of SERCA2a in heart failure. *Nature* **477,** 601–605
42. Ha, K. N., Masterson, L. R., Hou, Z., Verardi, R., Walsh, N., Veglia, G., and Robia, S. L. (2011) Lethal Arg9Cys phospholamban mutation hinders Ca^{2+}-ATPase regulation and phosphorylation by protein kinase A. *Proc. Natl. Acad. Sci. U.S.A.* **108,** 2735–2740
43. Shabb, J. B. (2001) Physiological substrates of cAMP-dependent protein kinase. *Chem. Rev.* **101,** 2381–2411
44. Minamisawa, S., Hoshijima, M., Chu, G., Ward, C. A., Frank, K., Gu, Y., Martone, M. E., Wang, Y., Ross, J., Jr., Kranias, E. G., Giles, W. R., and Chien, K. R. (1999) Chronic phospholamban-sarcoplasmic reticulum calcium ATPase interaction is the critical calcium cycling defect in dilated cardiomyopathy. *Cell* **99,** 313–322
45. Kass, D. A., Hare, J. M., and Georgakopoulos, D. (1998) Murine cardiac function. A cautionary tail. *Circ. Res.* **82,** 519–522
46. del Monte, F., Harding, S. E., Schmidt, U., Matsui, T., Kang, Z. B., Dec, G. W., Gwathmey, J. K., Rosenzweig, A., and Hajjar, R. J. (1999) Restoration of contractile function in isolated cardiomyocytes from failing human hearts by gene transfer of SERCA2a. *Circulation* **100,** 2308–2311
47. Paterlini, M. G., and Thomas, D. D. (2005) The α-helical propensity of the cytoplasmic domain of phospholamban. A molecular dynamics simulation of the effect of phosphorylation and mutation. *Biophys. J.* **88,** 3243–3251
48. Zamoon, J., Mascioni, A., Thomas, D. D., and Veglia, G. (2003) NMR solution structure and topological orientation of monomeric phospholamban in dodecylphosphocholine micelles. *Biophys. J.* **85,** 2589–2598
49. Knighton, D. R., Zheng, J. H., Ten Eyck, L. F., Xuong, N. H., Taylor, S. S., and Sowadski, J. M. (1991) Structure of a peptide inhibitor bound to the catalytic subunit of cyclic adenosine monophosphate-dependent protein kinase. *Science* **253,** 414–420
50. Masterson, L. R., Shi, L., Metcalfe, E., Gao, J., Taylor, S. S., and Veglia, G. (2011) Dynamically committed, uncommitted, and quenched states encoded in protein kinase A revealed by NMR spectroscopy. *Proc. Natl. Acad. Sci. U.S.A.* **108,** 6969–6974